Safe terrain probing method for multi-legged robots operating on brittle surfaces

Eranda Tennakoon[1 2], Navinda Kottege[2],
Thierry Peynot[1], and Jonathan Roberts[1]

[1] Science and Engineering Faculty, Queensland University of Technology
[2] Robotics and Autonomous Systems Group, CSIRO

Abstract. Multi-legged robots working in challenging environments are often required to walk on fragile terrain that may collapse upon traversal. We propose a method to test the robot's next foothold for collapses without endangering it. In this method, the robot's body is posed in a favourable manner and the terrain is probed to test for collapses using its foot. We also present a study in identifying collapses by using the force profile and the foot tip displacement of the probing foot during probing.

Keywords: Terrain probing, Legged robots, brittle terrain, terrain collapse

1 Introduction

One of the key use cases for autonomous robots is aiding in rescue missions [1]. Operating on such missions often require robots to traverse dangerous and difficult terrain [2]. This type of terrain often deforms upon traversal and puts the robot and its mission at risk. Therefore, the effectiveness of robots aiding in search and rescue operations largely depends on their ability to successfully traverse such terrain.

By design, legged robots offer a unique advantage on difficult terrain since they only require a series of small footholds as opposed to pathways or tracks. There have been some significant advances in legged robot locomotion on difficult terrain as demonstrated with BigDog [3] using whole body control to react to external disturbances, ANYmal [4] using pose optimisation to adapt to changing environments and Weaver [5] using adaptive methods to reduce the cost of transport on rough terrain. However, most of these methods are reactive methods that require the robot to enter potentially dangerous terrain before they can respond. This increases the overall risk as the robot may find itself in situations where it would be too late to recover and continue the mission or its actions would lead to damage. Therefore, it is useful to test the terrain before moving the robot into an area that can collapse.

The normal force exerted by a robot leg and the vertical foot displacement was related to the terrain stiffness by Kroktov in early work in this area [6]. Hoepflinger et al. [7] used robot terrain probing to determine terrain friction

and then predict terrain friction in un-traversed terrain using unsupervised machine learning methods. However, the use of terrain probing to determine terrain collapses has only received limited coverage in the literature. Tokuda et al. [8] using a pressure sensor on the sole of the robot's foot to show a change in the sensor voltage when the robot probes and incites a collapse at the foothold is one such example. Their study was limited to a laboratory model of collapsible foothold which they termed as a *breakable foothold*. Ambe and Matsuno [9] used the robot leg to probe the terrain to test if the foothold collapses under the exerted force. However, the method they use require them to set a threshold force to test on the robot leg to create the necessary constraints. This is not robust for real terrain situations as it is often not possible for the robot to test for a predefined threshold force. Furthermore, their method is not generalisable to robots with a greater number of legs as the problem of calculating foot contact forces becomes indeterminate when the robot has more than 3 legs in contact with the terrain [10].

In this paper, we introduce a novel terrain probing strategy for multi-legged robots operating on brittle terrain. Our approach is similar to [9] but is generalisable for any multi-legged robot and does not require the robot to meet a predefined threshold force. The proposed method moves the robot's centre of mass to a favourable location within it's support polygon to allow the robot to probe with more force while keeping the force applied on the terrain by the support feet below safe, pre-determined limits. We also show that we can classify whether terrain collapses occur on the brittle terrain by using the force profile and the foot tip displacement of the probing foot.

2 Method

We define that a terrain collapse has occurred when the robot's probing foot pierces through the brittle terrain layer and the foothold is no longer able to

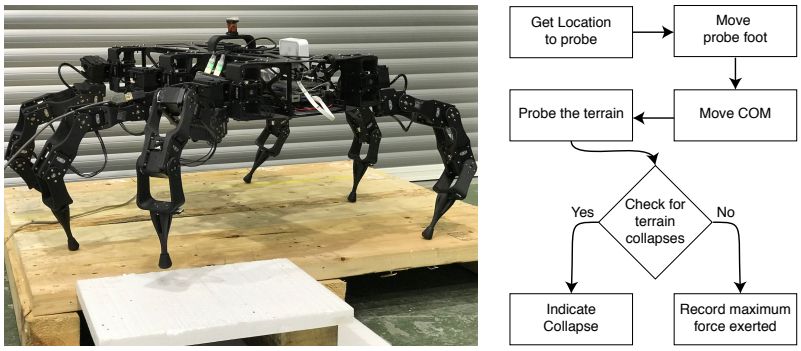

(a) (b)

Fig. 1. Hexapod robot Bullet probing a terrain sample (a) and the overview of the proposed method (b).

support the robot's weight component. If a collapse occurs during probing, this fact could be recorded and sent to a foothold planner so that it is taken into consideration in the next foothold planning process. If no collapse occurs during the probing, the maximum exerted force on the terrain is recorded and the robot can safely step on to the tested foothold. By keeping a record of these exerted maximum forces, a force restriction can be assigned to the particular foothold to keep the robot safe. In subsequent steps, the robot will need to make sure not to exceed this force restriction during motion since the foothold has not been tested to withstand a higher force.

We propose a method to effectively pose the robot's body (move the body without moving the feet) for one probing motion on the terrain. An overview of this method is shown in Fig. 1(b). First, the probing foot is moved on top of the foothold that needs to be tested, without making contact with it. Then the Center of Mass (COM) of the robot is posed strategically as proposed by our method. Finally, the robot is made to probe the given foothold and identify any collapses.

In this work, we assume that the robot is provided with a set of force restrictions on the robot's support feet which must not be exceeded during motion and an external footstep planner provides the robot with a feasible foothold that needs to be tested. Only the forces acting along the gravitational axis are considered since collapses are mainly inflicted by the robot's weight on the terrain. For simplicity, we assume that the terrain is locally flat (at the foothold) and does not break apart parallel to the surface and that it can withstand sufficient frictional force. The COM is assumed to be fixed at the body center of the robot and moves with the body center. The body of the robot is sufficiently heavy which restricts any large changes in the COM position.

2.1 Strategy for moving the COM and probing the terrain

The COM of the robot is posed iteratively towards a goal location using a gradient descent approach. A definition of the parameters and variables used are provided in Table 1. The outcome of the algorithm is a vector that determines the direction and the distance of movement of the COM for each iteration.

The potential to pose the COM towards a goal location is defined as $U_{goal} = \frac{1}{2}\epsilon\|O_{(c)} - O_{(g)}\|^2$. This drives the COM closer to the given goal at each iteration. The support polygon made up of the support feet (excluding the probing foot) will be referred to as the support polygon (SP) of the robot throughout this paper. The potential to keep the COM within SP is defined as $U_{polygon,i}$ for the ith polygon edge where $U_{polygon,i} = \frac{1}{2}\gamma(\frac{1}{\|O_{(c)} - O_{(p,i)}\|} - \frac{1}{D})^2$ for $\|O_{(c)} - O_{(p,i)}\| \leq D$, else $U_{polygon,i} = 0$. In the event of a terrain collapse during probing, this helps to keep the robot from stumbling or falling over. Any errors in the modelling of the COM position is also mitigated due to setting the threshold D.

To keep the robot from exceeding the force restrictions set on it, two potentials are defined. $U_{foot\,tip,j}$ pushes the COM away from the given foot tip (indexed as j) where $U_{foot\,tip,j} = \frac{1}{2}\eta(\frac{1}{F_{diff1,j}} - \frac{1}{F_{s1}})^2$ for $F_{diff1,j} \leq F_{s1}$, else

Table 1. Variables and parameters used

Variable	Definition
$O_{(c)}$	Current COM location
$O_{(g)}$	COM Goal location
$O_{(p,i)}$	Nearest point from the COM to the ith SP edge
$\|O_{(c)} - O_{(g)}\|$	Distance from the goal location to the COM
ϵ	Parameter imposing rate of potential change to goal
γ	Parameter imposing rate of potential change to SP edge
η	Parameter imposing rate of potential change to foot tip
β	Parameter imposing rate of potential change to SP edge force
D	Parameter for the safety distance to SP edge
$F_{current,j}$	Current force at foot tip j
$F_{rstrc,j}$	Tested force restriction value for foot tip j
F_{s1}	A safety force threshold for the foot tips
F_{s2}	A safety force threshold for each SP edge
$F_{diff1,j}$	$F_{rstrc,j} - F_{current,j}$
$F_{diff2,k}$	$(F_{rstrc,l1} + F_{rstrc,l2}) - (F_{current,l1} + F_{current,l2})$ where $l1$ and $l2$ are the two support feet that makes the kth SP edge

$U_{foot\,tip,j} = 0$. In some cases, the repulsion from two support feet can get mutually cancelled and the COM can move between the two support feet towards an SP edge (e.g. when the goal location for the COM is set outside the SP). When the COM moves towards an SP edge, the weight component on the two support feet making up that edge increases. Therefore, a virtual foot is defined on each SP edge at a point closest to the COM and a potential is defined similar to $U_{foot\,tip,j}$ using the force restrictions and the force values of the two support feet that makes each SP edge. $U_{polygonF,k}$ pushes the COM away from the SP edge (in terms of forces on the feet) where $U_{polygonF,k} = \frac{1}{2}\beta(\frac{1}{F_{diff2,k}} - \frac{1}{F_{s2}})^2$ for $F_{diff2,k} \leq F_{s2}$, else $U_{polygonF,k} = 0$.

The COM can be driven to a goal position by moving it in the direction of the greatest descent of the resulting potential field which can be calculated as $G = -\Delta U$ where U is the potential (specified above) and G is the gradient.

Using definitions for G and U_{goal} the gradient to the goal location can be calculated as $G_{goal} = -\epsilon(O_{(c)} - O_{(g)})$.

Similarly, the gradient from the ith polygon edge $g_{polygon,i}$, is calculated using $U_{polygon,i}$ (Eq. 1). The total rejection from the SP edge $G_{polygon}$ is then calculated using

$$g_{polygon,i} = \begin{cases} \gamma(\frac{1}{\|O_{(c)} - O_{(p,i)}\|} - \frac{1}{D})\frac{(O_{(c)} - O_{(p,i)})}{\|O_{(c)} - O_{(p,i)}\|^3}, & \text{if } \|O_{(c)} - O_{(p,i)}\| \leq D. \\ 0, & \|O_{(c)} - O_{(p,i)}\| > D. \end{cases} \quad (1)$$

and

$$G_{polygon} = \sum_{i}^{n} g_{polygon,i} \quad (2)$$

where n is the number of SP edges of the robot.

Finally, the gradient due to the force restrictions on the support feet can be calculated using the potential definitions $U_{foot\,tip,j}$ and $U_{polygonF,k}$ as follows:

$$g_{foot\,tip,j} = \begin{cases} \beta(\frac{1}{F_{diff1,j}} - \frac{1}{F_{s1}})(\frac{1}{F_{diff1,j}})^2 \frac{(O_{(c)} - O_{(f,j)})}{\|O_{(c)} - O_{(f,j)}\|}, & \text{if } F_{diff1,j} \leq F_{s1}. \\ 0, & F_{diff1,j} > F_{s1}. \end{cases} \tag{3}$$

$$g_{polygonF,k} = \begin{cases} \beta(\frac{1}{F_{diff2,k}} - \frac{1}{F_{s2}})(\frac{1}{F_{diff2,k}})^2 \frac{(O_{(c)} - O_{(p,k)})}{\|O_{(c)} - O_{(p,k)}\|}, & \text{if } F_{diff2,k} \leq F_{s2}. \\ 0, & F_{diff2,k} > F_{s2}. \end{cases} \tag{4}$$

The sum of their effect is then calculated using

$$G_{force\,restrictions} = \sum_{j}^{N} g_{foot\,tip,j} + \sum_{k}^{M} g_{polygonF,k} \tag{5}$$

where the number of support feet is given by N and the number of SP edges is given by M. The sum of the calculated gradient values given in Eq. 6 is a vector that determines the direction and the distance of movement of the COM for each iteration. This value is then mapped directly to the Cartesian plane.

$$G_{COM} = G_{goal} + G_{polygon} + G_{force\,restrictions} \tag{6}$$

However, at very large G_{COM} values the move distance for the COM will be very large. Therefore, the displacement vector (S) for the COM is defined as

$$S = \begin{cases} C\frac{G_{COM}}{\|G_{COM}\|}, & \text{if } G_{COM} > C \\ 1 & G_{COM} \leq C \end{cases} \tag{7}$$

Here, C is a constant that is decided experimentally considering the minimum move distance of the COM allowed by the *robot controller* (controller responsible for moving the COM of the robot to the desired location) and the number of move iterations typically required to move the COM to a given goal.

After the COM is moved to a favourable location for the probing action, the probing foot is lowered in a direction normal to the foothold surface along the gravitational axis. The probing motion is ended when either of the following 3 conditions are reached: 1) the probing foot reaches the torque limit of any of its motors, 2) the workspace limit of the probing leg is reached, or 3) one of the support feet lifts off the ground (e.g. when the robot tilts back when pushing on the probe point).

2.2 Identifying terrain collapses

Thanks to the probing action, we want to classify whether the terrain at the given foothold belongs to the class *collapse* and *non-collapse*, i.e. we want to determine whether the terrain at a given foothold collapses or not. A set of features were chosen experimentally from the force profile of the probing foot

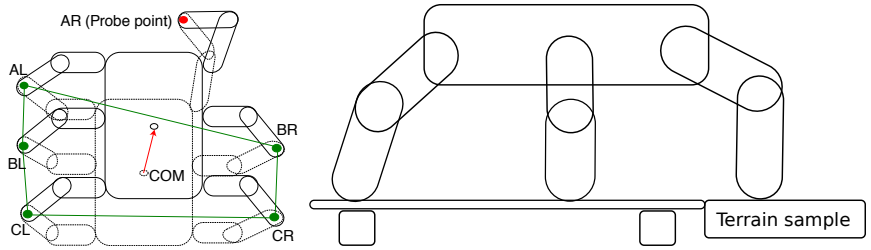

(a) (b)

Fig. 2. COM moved by posing the robot within the SP (top view). Legs were named AR,BR,CR,CL,BL and AL clockwise (a). Illustration of robot probing (side view) (b).

and the probing foot position relative to the robot body during probing. These selected features are: 1) the maximum force recorded during probing (F_{max}), 2) the foot tip travel distance from the start of probing motion at F_{max}, 3) the maximum foot tip travel distance from the start of probing motion to the end, 4) the force at the foot tip at the end of probing, and 5) the torque at each motor of the probing leg at F_{max}. A classification is performed to determine whether the chosen feature vector allows the robot to classify the occurrence of terrain collapses effectively. The reference labelling of terrain samples used for training and for testing is based on the observation whether a collapse occurred or not during probing, made by an expert.

3 Experiments and setup

The experiments were done using the hexapod *Bullet* (Fig. 1(a)). Bullet has 5 degrees of freedom in each leg and has the configuration *yaw-pitch-roll-roll-roll*. The links and corresponding joints are named Coxa (with a yaw and a pitch joint), Femur, Tibia, and Tarsus. The specifications for the robot and computer used are given in Table 2. For the experiments in this section, we used the following values for the parameters of our proposed method: $\epsilon = 0.02\, Jm^{-2}$, $D = 0.12m$, $\gamma = 1.3925 \times 10^5\, Jm^2$, $\eta = 2.67 \times 10^7\, JN^2$, $\beta = 4.25 \times 10^6\, JN^2$, $F_{s1} = 0.05N$ and $F_{s2} = 0.1N$.

Table 2. Hardware Specifications of Bullet hexapod and the computer used.

Type	Description
General	Mass: 9.51 kg Dimensions (Body): length = 500 mm × width = 280 mm
Servomotors	30 × Dynamixel MX-106
Computer	Intel core i5 PC (16 GB RAM) running ROS on Ubuntu 16.04

3.1 Experiment 1: Moving the COM

We first test how the proposed method moves the COM to a given goal location. Ideally, the robot is able to exert the most force when the COM is moved right on top of the probe point (i.e. weight vector going through the probe point). However, the COM movement is restricted to within the SP and therefore, the COM needs to be moved to a favourable location within the SP. One such favourable location is the closest point to the probe point from within the SP as it gives a higher weight component of the robot on to the probe point [11]. We set the goal location as the probe point itself. This moves the COM to the desired favourable location and at the same time allows to test how the method responds to goal locations outside the SP. For simplicity, the COM is moved assuming that the probing leg is connected to the body center of the robot at a point with no offset and the probing point was chosen such that the effects of this offset on the robot probing are minimized. No force restrictions were set on the support feet for these experiments. Figure 2(a) shows the initial position of the COM of the robot with the COM moved to a final position by posing the robot body.

Next, two sets of tests were performed to study the system's ability to handle force restrictions on the support feet. We are aiming to use the maximum probing force exerted on the foothold as the force restriction (section 2). However, for the purpose of testing the method, simulated force restrictions were set on the support feet for these experiments. In the first test, a force restriction value was set to only one of the legs to see how the method behaves. The leg that was closest to the probing point (arbitrarily selected) was chosen to set the force restriction to highlight the effects.

In the second test, a random set of force restrictions were set on all the support feet. The random force values were generated ensuring that the robot was not starting off with invalid initial conditions. The robot was then made to move with the given force restrictions using the proposed method. The robot was also made to do a probing on a known (by an expert) collapsible terrain sample. This was done when the robot was at the final COM position after moving with the aforementioned random force restrictions.

3.2 Experiment 2: Identifying terrain collapses

In this experiment, we performed a simple study of identifying terrain collapses. The robot was made to probe a point within the workspace of the probing leg where we place different terrain samples. To simplify the experiment and to allow the robot to probe with the same initial conditions, the robot's COM was not moved in these experiments and the probing was done with the robot at its initial pose. Based on the previous experiment we chose the probe point such that the robot's COM was close enough to exert a considerable force, yet not too close to lose generality. However, in the actual implementation, this step can be done after the robot has moved the COM to a favourable location.

The samples in Table 3 were chosen for their common occurrence in urban environments as well as easy repeatability of experiments. Figure 2(b) shows

Table 3. Terrain samples

Non-collapsible	Collapsible
Brick	Damp peat slab
Hardwood	Thin ice
Hard ice	Styrofoam (5 mm)
Styrofoam (15 mm)	Styrofoam (10 mm)
Gravel	

how the robot is made to probe a collapsible terrain sample. After the robot probes each sample, the force profile at the foot tip and the foot tip position (relative to the robot center) were recorded. The features were extracted from the data and then labeled as *collapse* or *non collapse* depending on the result of the probing. A simple binary classification was done using a Support Vector Machine (SVM). A comparison of classification accuracy was also done using discriminant analysis and k-nearest neighbours to evaluate the discrimination power of the chosen feature vector with different classifiers.

4 Results and analysis

4.1 Results and analysis of Experiment 1

The robot was made to probe the chosen point in the terrain after each movement of the COM (for each iteration of the gradient descent algorithm). Fig. 3 shows the force at the foot vs. the distance between the COM and probe point for five trials along with a least squares fitted curve (Polynomial of degree 3). In the first iteration of the gradient descent (in each run of the experiment), the probing motion was ended because the probing leg reached the workspace limit. In the remaining iterations, the probing motion was ended by the robot's feet (AL and BR which are closest to the probing foot) lifting off the platform. The force required to lift the support feet increased at each movement of the COM

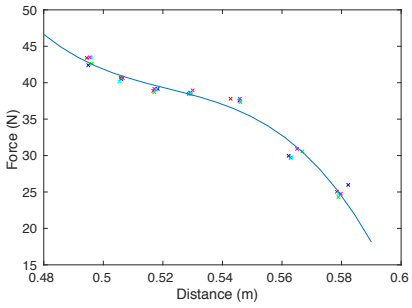

Fig. 3. Maximum force calculated at each probe for each movement iteration of the COM vs. distance from the probe point to the COM for multiple runs of the experiment (shown in different colours). A curve fitting was done to show the variation.

indicating that the selected goal location for the COM position is favourable as each iteration transferred more weight of the robot onto the probing foot.

In Fig. 4(a) the movement of the COM (relative to the initial SP) for one of the experiment runs in Fig. 3 is presented. Here, the movement of the Coxa joint with the COM indicates that both points came closer to the probe point at each iteration and thereby minimizing any effects that could be introduced by the offset. The amount of weight the robot transfers to the probing leg is decided by the position of the COM, but the amount of force it can exert on the terrain can be limited by the distance from the probe point (probe leg's point of contact with the terrain) to a given joint in the probing leg as well as the orientation of each joint. Examining the effects of those aspects on the probing force is beyond the scope of this study. However, a new goal location for the COM can easily be set by considering the effects of the aforementioned aspects. It was also observed that the initial and final shape of the SP was different due to position errors of the legs. The proposed gradient method approach was robust to these errors as the new SP was calculated and considered for the algorithm in each iteration.

Next, moving the COM with force restrictions was tested by first imposing a force restriction only on one foot. The Fig. 4(b) shows the COM movement when different force restrictions were set on just one foot. Here, the feet of the robot is marked as AR, BR and CR on the right-hand side and AL, BL, and CL on the left-hand side. In this case, AR is the probing foot marked as *probe point* in the Fig. 4(b) and BR is the support foot with the force restriction imposed. As the force restriction on the BR foot gets more strict, the COM was pushed further away from the foot. Fig. 5(a) shows the force profile of the BR foot for the force restriction of 21 N set on it compared with the force profiles of all the support feet. It can be observed that the BR foot always stayed under the imposed force restriction which was the goal of the proposed method.

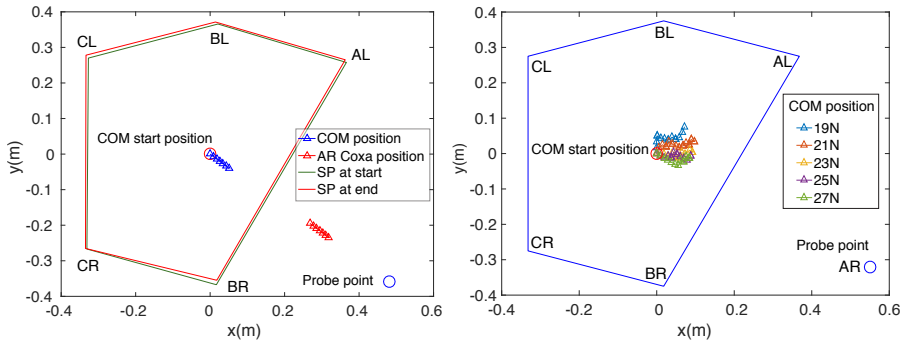

(a) (b)

Fig. 4. COM movement during probing relative to the initial SP, with (a) showing COM movement with no force restriction on any foot and (b) showing COM movement for five trials, each with a unique force restriction set on the BR foot.

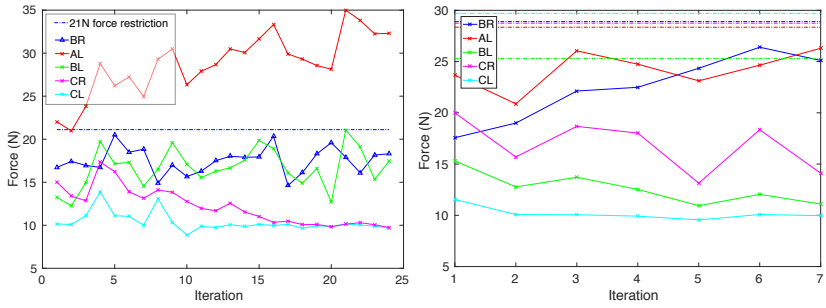

(a) (b)

Fig. 5. Force profile with each iteration with force restriction set to 21 N is shown in (a) and the force profile of support feet with each iteration of COM movement with random force restriction on support feet is shown in (b). The dashed lines represent the force restriction for each respective foot.

Fig. 5(b) shows the force profile of each support foot at each iteration when random force restrictions were set to all of the support feet. The proposed strategy was successful in moving the COM of the robot within the SP while not exceeding the imposed force restrictions. The force profile of the closest feet to the probe location kept increasing gradually as expected when the COM came close to the SP edge. To demonstrate the intended final outcome of the proposed method a simple probing was done on a Styrofoam piece once the robot reached the final COM position with the given force restrictions. Figs. 6(a) and 6(b) show the force profile of the probing foot and support feet respectively while probing the Styrofoam piece (collapsible foothold). Clear changes were observed at the collapse point in the force profiles of the probing foot and the support feet. The probing was done ensuring that the force restrictions on the support feet were not exceeded (Fig. 6(b)).

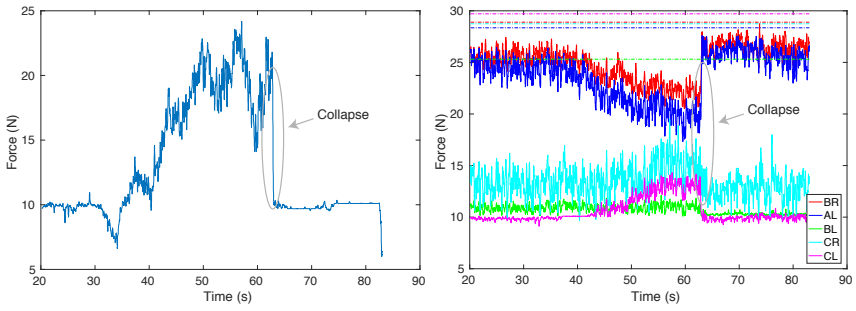

(a) Force at the probing foot (b) Forces at the support feet

Fig. 6. Forces at the feet when the robot was probing a Styrofoam piece.

Table 4. Classification for a material not in the training data using different classifiers.

Label	Material	SVM	DA	KNN
Collapse	Thin ice	4/5	5/5	5/5
	Styrofoam (5mm)	5/5	5/5	5/5
	Styrofoam (10mm)	4/6	6/6	6/6
	Damp peat slab	5/5	5/5	5/5
Non Collapse	Brick	5/5	5/5	5/5
	Gravel	4/5	4/5	4/5
	Hard wood	5/5	5/5	5/5
	Styrofoam (15mm)	4/6	6/6	6/6
	Hard ice	5/5	5/5	5/5

4.2 Results and analysis of Experiment 2

Based on the terrain probing, a study of the terrain collapses was done using simple classification methods. A total of 47 terrain samples were tested and the features were labeled as *collapse* or *non-collapse* depending on the outcome of probing. The trials were separated 50/50 for the training set and the test set by random sampling of the data. An F1 score of greater than 0.88 was obtained for multiple experimental runs evaluated with a support vector machine (SVM) classifier (with a Gaussian kernel), indicating good classification results.

Next, the chosen set of features was evaluated for its ability to classify the occurrence of terrain collapses on previously unobserved terrain data. For this analysis, one of the terrain materials was left out of the training data and the classifier was made to classify this as a collapse or a non-collapse based on the training done on the remaining data. This binary classification was done using the 3 classifiers: SVM, discriminant analysis (DA) and k-nearest neighbours (KNN). Table 4 shows the number of samples each classifier correctly labeled against the number of samples tested. From the results, we see that all the classifiers managed to correctly classify the majority of the samples. This indicates that the chosen feature vector performs well for identifying terrain collapses.

5 Conclusion

We presented a terrain probing method to aid legged robots to safely identify terrain collapses on brittle terrain. This method was shown to be robust to position errors of the leg joints as the COM was moved within the support polygon of the robot's support feet to allow more force to be exerted on the terrain. The COM movement is executed without exceeding the predetermined force restrictions at the robot's support feet. This indicates that the proposed method is applicable in real terrain conditions where the robot's ability to effectively probe the terrain is compromised. It is especially relevant when the robot is already on brittle terrain with the risk of collapse if additional force is exerted on support feet while probing terrain ahead.

A simple binary classification of terrain collapses was also performed using the force profile and the foot displacement of the probing foot. The chosen feature

vector comprising the force profile and the foot tip displacement of the probing leg was shown to be effective in determining whether terrain collapses occurred during probing.

In future work, we plan to extend the proposed method to a continuous gait (probe before step) that also takes lateral forces on the probing leg into consideration to gain further information about the terrain.

Acknowledgements

The authors would like to thank Fletcher Talbot, James Brett, Pubudu Aravinda and Benjamin Tam for their support during this work.

References

1. Murphy, R.R., Tadokoro, S., Nardi, D., Jacoff, A., Fiorini, P., Choset, H., Erkmen, A.M.: Search and Rescue Robotics. In Siciliano, B., Khatib, O., eds.: Springer Handbook of Robotics. Springer (2008) 1151–1173
2. Messina, E., Jacoff, A., Scholtz, J., Schlenoff, C., Huang, H., Lytle, A., Blitch, J.: Statement of requirements for urban search and rescue robot performance standards. Draft report, DHSSTD and NIST, USA (2005)
3. Raibert, M., Blankespoor, K., Nelson, G., Playter, R.: Bigdog, the rough-terrain quadruped robot. IFAC World Congress **41**(2) (2008) 10822 – 10825
4. Hutter, M., Gehring, C., Jud, D., Lauber, A., Bellicoso, C.D., Tsounis, V., Hwangbo, J., Bodie, K., Fankhauser, P., Bloesch, M., Diethelm, R., Bachmann, S., Melzer, A., Hoepflinger, M.: ANYmal - a highly mobile and dynamic quadrupedal robot. In: IEEE/RSJ International Conference on Intelligent Robots and Systems (IROS). (2016) 38–44
5. Bjelonic, M., Kottege, N., Homberger, T., Borges, P., Beckerle, P., Chli, M.: Weaver: Hexapod robot for autonomous navigation on unstructured terrain. Journal of Field Robotics (2018)
6. Krotkov, E.: Active perception for legged locomotion: every step is an experiment. In: IEEE International Symposium on Intelligent Control. (1990)
7. Hoepflinger, M.A., Hutter, M., Gehring, C., Blösch, M., Siegwart, R.: Unsupervised identification and prediction of foothold robustness. In: IEEE International Conference on Robotics and Automation (ICRA). (2013) 3293–3298
8. Tokuda, K., Toda, T., Koji, Y., Konyo, M., Tadokoro, S., Alain, P.: Estimation of fragile ground by foot pressure sensor of legged robot. In: IEEE/ASME International Conference on Advanced Intelligent Mechatronics (AIM). (2003) 447–453
9. Ambe, Y., Matsuno, F.: leg-grope walk: strategy for walking on fragile irregular slopes as a quadruped robot by force distribution. ROBOMECH **3**(1) (2016)
10. Schmucker, U., Schneider, A., Rusin, V., Zavgorodniy, Y.: Force sensing for walking robots. In: International Symposium on Adaptive Motion of Animals and Machines (AMAM). (2005) 25–30
11. Garcia, J., Wood, G., Barrera-Mora, F.: Reactions on rigid legs of rectangular tables. Applied Mathematics **6**(03) (2015) 599